Estimation of through-plane and in-plane gas permeability across gas diffusion layers (GDLs): Comparison with equivalent permeability in bipolar plates and relation to fuel cell performance

Mainak Mukherjee, Caroline Bonnet, François Lapicque

Estimation of through-plane and in-plane gas permeability across gas diffusion layers (GDLs) : comparison with equivalent permeability in bipolar plates and relation to fuel cell performance

Mainak Mukherjee [a], Caroline Bonnet [a], François Lapicque [a]*

[a] Laboratoire Réactions et Génie des Procédés, CNRS-Université de Lorraine, 1 rue Grandville, 54000 Nancy, France

Abstract

The present work focusses on measuring the permeability across gas diffusion layers (GDLs) first in a dedicated cell and later in PEM fuel cell configuration with varying bi-polar plate designs. Eight carbon paper-based GDLs with and without the microporous layer (MPL), have been tested. An in-house designed dedicated cell allowed measuring pressure drop depending on flow rate, for i) through-plane and ii) in-plane direction. Further, transport measurements were conducted in 25 cm^2 bi-polar plates (BPs) in fuel cell configuration having single or multiple serpentine channels, by stacking the GDL inside. The results show that gas permeability in the dedicated cell for through-plane and in-plane can be estimated by using Darcy's law. However, for BPs, the flow is affected additionally by inertial contribution (Darcy-Forchheimer). Finally, the efficiency allowed by selected GDLs installed in a fuel cell under operation shows a relationship between the equivalent permeability and the fuel cell performance.

Highlights:

- Measured through- and in-plane permeability of GDL in a specially dedicated cell.
- Measured the equivalent permeability of GDLs in bipolar plates of PEM fuel cells.
- The equivalent permeability of GDL greatly differs from those obtained in a dedicated cell.
- Inertial flow in the GDL stacked between the bipolar plates is of appreciable significance.
- Relationship between equivalent permeability and fuel cell performance.

Keywords: Proton exchange membrane fuel cells; Gas diffusion layers; Through-plane permeability; In-plane permeability; Equivalent permeability

Corresponding Author: Dr. François Lapicque francois.lapicque@univ-lorraine.fr

1. Introduction

With the advancement in renewable energy technologies, and thereby understanding its need for the future, proton exchange membrane fuel cells (PEMFCs) have gained major attention. PEMFCs as energy devices actually exhibit some interesting features like a fast start-up, high working efficiency, ease in operation and zero-emission [1-6]. These features collectively enable the PEMFCs for a large number of applications, such as in automobiles or in combined heat and power generation to mention a few. Essentially, improvements associated with PEMFC technology are still in progress, following to which increased performance and durability with a cost reduction, are expected [2-8].

In PEMFCs, fed gases have to pass through a carbon-based porous layer i.e. 'gas diffusion layer' (GDL) for access to the catalyst layer, thereby making the electrochemical reaction possible and the subsequent energy production. Positioned between the bipolar plate and the catalyst layer, the GDL exhibits thermal and electrical conductivity and allows gas and water transport. The GDL substrate also known as macroporous substrate (MPS) forms the primary structure with pore sizes ranging from 10 to 30 µm and per nature is highly anisotropic. With the advent of technology, GDLs have been developed for stricter operations such as balancing of hydration level in the membrane and working under varying load conditions to meet demands. For this purpose, an additional microporous layer (MPL) with pore size in the range 50-500 nm is often deposited onto the MPS: its degree of hydrophobicity can be adjusted at the targeted value by polytetrafluoroethylene (PTFE) loading in addition to the water-repellent carbonaceous compounds of the MPL [1,5,8]. The MPL typically provides a smoother layer with a finely divided surface, which facilitates efficient contact with the catalyst layer. The MPL in a GDL assists in water management by expelling excess water accumulated in the GDL-catalyst layer interface, thus maintaining suitable hydration levels. [2,5].

Gas transport of reactants across GDLs is both through-plane and in-plane in fuel cells as explained below. Through-plane transport refers to transport perpendicular to the plane of the GDL and the membrane electrode assembly (MEA), from the gas channel to the electrode. In-plane transport corresponds to gas flow parallel to the above planes: this may occur when the gas is transported over a rib (by-passing flow, also referred to as under-land crossflow) to reach the neighbouring channel.

The permeability of a porous medium is the ability of the medium to facilitate the flow of fluid through its open pores. Gas diffusion layers used in fuel cells exhibit broad pore size

distributions, high anisotropy, and appreciable tortuosity [2,4,5]. Lately, permeability measurements across GDLs placed in PEMFCs have gained prominence in the pursuit of achieving higher working efficiency. Higher permeability of gas across the GDL would lead to a superior reaction at the catalytic site [2,6,9,10]. In general, for low gas flow velocities in a single phase, Darcy's Law is used to describe the flow through a porous media. In fluid flow, viscous forces are the inherent forces that resist the flow of a fluid: these forces predominate in the laminar flow regime. However, as the flow velocity increases across the porous media i.e. the GDL, inertial forces can become significant [9,10]. This introduces the concept of viscous and inertial permeability, the latter appearing in Darcy-Forchheimer's law, in which the inertial term in the momentum balance is accounted for. Inertial permeability values of GDL are nevertheless seldom reported [9].

In-plane and through-plane permeability largely depend on the intrinsic properties of GDL such as thickness, density, PTFE deposition, anisotropy degree, and the presence of MPL to mention a few [2,8,11,12]. Various techniques have been developed in dedicated cells for the determination of the permeability across GDLs [2,4,5,9,13,14]. Viscous permeability values reported for a fresh sample of SGL 24 BC comprising an MPL taken from different batches were found to be 1.46×10^{-13} m^2 and 5.96×10^{-14} m^2 , i.e. with a 2.5 factor between the two values. It was also concluded that the variation in the permeability values might be caused by the unevenness during fabrication stages [9], or by different compression states [6, 15,16]. The impact of the MPL was formerly studied: it was found that the permeability across the MPL is approximately two orders of magnitude lower than that of the MPS [4,17]. Furthermore, in-plane permeability measurements showed the presence of inertial forces in the MPS leading to the Forchheimer effect [2]. In addition, carbon paper-based GDLs showed a higher in-plane permeability compared to their through-plane permeability [2]. Moreover, through-plane viscous permeability of several Toray samples was observed to decrease upon an increase in PTFE content [10]. However, permeability values of aged GDLs are also affected by the occurrence of e.g. local compression leading to rupture (while assembling and long usage of the fuel cell), erosion (washing-out of the MPL), and water accumulation caused by loss of MPL [1,6,8,16,18].

In PEM fuel cells, gas flow in a GDL is subjected to a force balance between the free convection in the channel and the above through-plane and in-plane transport, depending on the GDL properties, the channel dimensions, and the flow pattern. The occurrence of water slugs in the MPS or in the channel is to change this balance, then the significance of each

transport phenomenon [19,20]. In particular, the significance of by-passing flow (or under-land cross-flow) in single serpentine configuration has been investigated by various modelling works or by experimental determination [20-22]. This side transport phenomenon corresponding to in-plane transport was shown to be significant for GDL through-plane permeability larger than 10^{-13} m^2 [20], which is the case of most macroporous GDLs. Besides, whereas predominance of viscous flow has been mentioned in many papers e.g. [9], more dedicated investigations showed that Darcy's law cannot predict the pressure gradient in the GDL upon by-passing flow [20,23], then evidencing appreciable contribution of inertial flow in by-passing flow. According to [23], this contribution could also be linked to the quadratic expression of the pressure drop with the gas velocity in bendings and U-turns of the flow channel. However, a question rarely addressed is whether the in-plane and through-plane permeabilities measured in specific cells whose dimensions and flow conditions largely differ from those in real fuel cells, are relevant to express, at least in a phenomenological manner, gas transport from the channel to the catalytic layer in a fuel cell under operation. To our knowledge, no such experimental data have been reported so far.

For this purpose, the present study deals with two specified aspects concerning the experimental determination of i) in-plane and through-plane permeability by using an in-house dedicated cell with paper-based GDL samples, with and without MPL, and ii) the GDL permeability following a similar measurement approach in a 25 cm^2 fuel cell configuration (not operating), with different flow patterns of their bipolar plates (BP). For this purpose, a simple GDL sheet was placed between the two bipolar plates to emulate gas transport from the channels (here one BP) to the catalyst layer (here the other BP). The aim of this overall approach was to observe whether values for the permeability determined in a dedicated cell could be representative of the permeability of the GDL stacked between two BPs, i.e. whether the usually reported permeability values could be used in a model for gas transport in a fuel cell, from the channel to the electrode. After the description of the experimental bench, the materials used and the theory used for measurement interpretation, permeability data of the selected GDLs in the two measurement devices have been presented and discussed. Finally, the efficiency allowed by the selected GDLs installed in a fuel cell under operation in terms of cell voltage at high current density could be related to the permeability value.

2. Experimental section and methodology

2.1. Measurement method

Permeability of GDLs provided with and without MPL, using pure nitrogen, has been determined in a dedicated cell, whose design allows investigation of either through-plane or in-plane flow across the GDLs, and also through the GDL stacked between two BPs. In both cases, the GDL samples were installed between two compartments: nitrogen fed at a controlled flow rate was transported through the GDL structure for its possible evacuation from the cell. The fundamental cell developed and the fuel cell designs used are further described in sections 2.2 and 2.3 respectively.

To control the flow rate across the gas diffusion layer, a mass flow controller (Brooks Instrument 0245) was installed. Test runs were performed initially, and leak-proofing was conducted. The pressure drop was measured using a differential pressure transmitter (Keller Pa 23/25) (max. pressure difference = 200 mbars) at the entry and exit of the cell respectively. For pressure differences below 1 mbar, a lower range pressure sensor (Keller series 23 SY) and indicator (Newport INFCP1) were used. The pressure drop across the tested GDL samples was measured depending on the flow rate in both the dedicated cell and the bipolar plates of fuel cells. The gas flow rate at the outlet was measured with a difference from the inlet flow rate, usually found below 3%. The outlet value was considered for the interpretation of the data. The ambient temperature and pressure were noted for all the runs for estimation of the gas viscosity η and density ρ.

An error study on bench setup was carried out to find the margin of error in the permeability measurements. Individual accuracy for each device and GDL sample was either measured manually or was taken from the technical specification sheet. To find the repeatability and uncertainty of the experimental data, experiments were replicated at least for 3-4 times. For the selected GDLs, relative uncertainty percentage was usually estimated around ($\pm$ 5 – 8 %). This uncertainty could be larger for one GDL, for which the pressure difference was below 1 mbar even with the highest flow rates.

2.2 Design of the fundamental cell for through-plane and in-plane measurements

An in-house measurement cell, named as the fundamental cell was designed for the determination of ‘in-plane’ and ‘through-plane’ permeability values independently. The fundamental cell has a configuration of a top and a bottom assembly shown in Figure 1 (a-c). On the top assembly, there is an inlet port for gas entry with a diameter of 5 mm. On the bottom assembly, two outlet ports for in-plane and through-plane gas exit having a diameter of 5 mm each were constructed. The GDL disk of 20 mm in diameter stacked between the two

assemblies, resides upon a 20 mm circular groove. In through-plane configuration (in-plane outlet closed), the gas flowing in the cell is exposed to the ⌀ 5 mm MPS surface of the GDL and flows perpendicularly through the GDL. With in-plane configuration (through-plane outlet closed), the gas flows radially from the inner radius (R_i = 2.5 mm) to the outer radius (R_e = 10 mm). The flow rate of gas was varied in this cell in the range of 10 -150 NmL/min.

The pressure downstream of the GDL sample was in all cases at ambient level P_0. The torque applied by using the wrench on the screws was at 1 Nm for sufficient fastening without damaging the GDL sample, as developed in preliminary tests. An external silicon gasket with a thickness of 2.60 mm ensured no gas leakages.

2.3 Permeability measurements in the bipolar plates for fuel cells

Two differently designed 25 cm^2 bipolar plates for fuel cells (Electrochem) were deployed for estimating the permeability in the GDLs stacked between the bipolar plates: this permeability does not refer exactly to through-plane or in-plane transports, but can be considered as an equivalent property of the GDL in such conditions. The bipolar plates were made from graphite materials. Two differently designed bipolar plates were used:

- The first cell has a single serpentine flow channel (1.3 mm wide and 1 mm deep) with a total length of 102.9 cm and 20 bends.
- The second cell with parallel channels (0.6 mm wide, 0.6 mm deep) was referred to as a multi-serpentine flow channel. In this cell, there are 7 clusters with each cluster allocated with 5 channels.

As shown in Table 1, the surface area of the channels, $S_{channel}$, was equal to 13.1 cm^2 for the single serpentine pattern and 16.2 cm^2 for the multiple serpentine patterns. A squared sample of GDL was stacked between the two plates of the same–pattern: its dimensions exceeded slightly the grooved area to avoid leakage. The cell was fastened at 3.5 Nm as in real cell operation with an MEA. A silicon gasket with thickness in accordance with that of the GDL was positioned surrounding the GDL for complete leak proofing.

The flow rate of the gas during this measurement varied from 0 to 1.0 NL/min as explained below. This range can be compared to the flow rates of reacting gases in the 25 cm^2 cell under operation. Consider the cell operating at 1.0 A/cm^2, the flow rate of air-simulating gas for complete oxygen consumption at the cathode is near 0.41 NL/min, which justifies the above range.

2.4 GDLs used for the measurements

The selected paper-based GDLs (Sigracet-Germany) used are presented in Table 2. Amongst the eight GDLs employed, only two (24 AA and 28 AA) were not impregnated by polytetrafluoroethylene (PTFE). The six others form two groups of GDL, two without MPL (grade BA), the other GDL (grade BC) derived from the BA grade by further deposition of an MPL. The difference between the various groups (24, 34, 28 and 38) is related to the MPS thickness and porosity, with a diameter of carbon fibers near 8 µm for more ancient grades 24 and 34 [2]. PTFE-free substrates AA exhibit slightly larger porosity (Table 2), corresponding to the fact that fibers are not linked to each other by the water-repellent polymer. The presence of MPL in grades 24 BC and 34 BC makes them highly compact, resulting in overall lower porosity (Table 2) than for macroporous substrate grades.

2.5 Performance of GDL-MEA in real fuel cell under actual working conditions.

Following the different permeability estimations of the selected GDLs, an attempt at understanding its effect on the fuel cell performance was made. In the set of measurements, considering four different MPL-protected GDLs (Table 2) were used individually alongside an MEA formed by a Nafion 212 membrane and two catalyst layers (Pt/C 70% - 0.5 mgPt/cm^2) (Paxitech). The prepared assembly for the case of each GDL was installed in the fuel cell provided with multichannel flow pattern BPs (Section 2.3). Tests were carried out at 55°C, at a pressure close to the ambient level, with stoichiometric factors for hydrogen and air at 1.3 and 3 respectively. Only air was humidified at 50%. To draw a fair comparison of the GDLs-MEA, the cell was first operated at 0.4 A/cm^2 for four hours so that a perfectly steady voltage could be obtained, following to which chronopotentiometric measurements were carried out with 20 min voltage measurements for each current density value in the range of 0-1 A/cm^2.

3. Theory for data interpretation

During measurements, firstly the fuel cell setup was installed without the GDL, and the pressure drop caused by the flow in “empty” cell structure was recorded at various flow rates. Then, measurements were conducted with the GDL stacked between the bipolar plates. The actual pressure drop related to gas transport through the GDL was obtained by subtracting the pressure drop without the GDL from those measured with the GDL.

3.1. Gas velocity in the fundamental cell

The velocity of the gas v is related to its flow rate Q at working P and T conditions taking into account the cross-sectional area of the system. For through-plane measurements, this area is defined on the basis of radius R_i whereas, for in-plane transport, the gas velocity varies continuously with the radial coordinate r from R_i to R_e as shown later in Figures 2 and 5. Thus:

$$v(r) = \frac{Q}{2\pi L r} \qquad (1)$$

where L is the thickness of the GDL.

In the general case of compressible gases, velocity and flow rates are related to pressure P and can be expressed to their corresponding values, $v_{0,}$ and Q_0 respectively at ambient pressure P_0 and working temperature T.

For through-plane measurements, the flow range considered and given in section 2.2, corresponds to maximum velocity v_0 near 13.6 cm/s, which is far beyond the gas velocity through the GDL in fuel cells. For in-plane measurements, the amount of gas flowing is quantified by the average velocity in the disk at ambient pressure, $v_{av,0}$. This velocity is calculated by integration of Eqn.1 between R_i and R_e at ambient pressure, and taking into account the radial distance (R_e-R_i): the following expression can then be yielded:

$$v_{av,0} = \frac{Q_0}{2\pi L\left(R_e - R_i\right)} Ln\frac{R_e}{R_i} \qquad (2)$$

For instance, in a 230 µm thick GDL, the maximum flow rate fed corresponds to an average velocity of the gas $v_{av,0}$ near 34 cm/s.

3.2. Flow and average gas velocity in the fuel cell

In a fuel cell under operation, the gas flows in the BP channels and is transported to a part to the catalytic layer through the gas diffusion layer. As expressed above, depending on the BP design, the GDL properties and the compression level, access to the catalyst layer covers various transport phenomena, including direct flow through the GDL and channel by-passing (Figure 2a, only one chamber is drawn for the sake of simplicity). To emulate the overall transport for the reacting gas from the flow channel to the catalyst layer, the investigated GDL was stacked between two bipolar plates. As shown in Figure 2b, the gas passes from the left-hand chamber to the right side through the GDL, according to the phenomena mentioned above. Because of the complexity of physical phenomena occurring in the GDL, the

experimental data of pressure drop vs. flow rate have been treated considering the average velocity v_0 of the gas on the basis of the channel area, $S_{channel}$, assuming in the approach that the gas flows normally (through) the GDL structure (Figure 2c). As a matter of fact, the part of the GDL appearing in dark in Figure 2c represents the considered area with nil gas transport, following the assumption made here. Depending on the flow pattern considered, the gas flow rate emulating full air oxygen consumption at 1 A/cm^2 corresponds to gas velocity v_0 equal to 0.53 and 0.43 cm/s for the single-channel and multiple channel flow patterns respectively.

Although an overall method, and because mimicking the various transport phenomena in the cell under operation at their actual rates is virtually impossible, the approach has been selected for estimation of the equivalent permeability of the GDL when stacked in the bipolar plates tested.

3.3. Estimation of GDL permeability

The permeability of gas across the GDLs placed in the fundamental cell and in the real fuel cells were calculated separately.

Darcy's law Eqn.3, states that the pressure gradient is directly proportional to the fluid flow rate [2,4,12,13], then, for a one-dimensional system (coordinate x):

$$\frac{dP}{dx} = -\left(\frac{\eta}{K_v}\right)v \qquad (3)$$

where η is the viscosity of the fluid in Pa s, K_v is the viscous permeability in m^2 and v is the local velocity at P across the porous media in m/s.

- For through-plane flow, integration of Eqn.3 through the layer yields:

$$\frac{P_{in}^2 - P_{out}^2}{2LP_0} = \frac{P_{in}^2 - P_0^2}{2LP_0} = \left(\frac{\eta}{K_v}\right)v_0 \qquad (4)$$

where P_{in} is the gas pressure upstream of the GDL sample, after deduction of the empty cell contribution. The group $\left(\left(P_{in}^2 - P_0^2\right)\Big/2LP_0\right)$ can be considered as being the overall pressure gradient in the GDL for through-plane transport.

- For the case of in-plane permeability, Eqns.1 and 3 yield a differential equation whose integration leads to:

$$\frac{P_{in}^2 - P_0^2}{2(R_e - R_i)P_0} = \left(\frac{\eta}{K_v}\right) v_{av,0} \qquad (5)$$

The left-hand term in Eqn. 5 represents the overall pressure gradient for in-plane transport in the GDL sample.

However, as the flow velocity increases, an inertial term has to be added to Darcy's law, yielding the Darcy-Forchheimer equation (6) [9,12,16]:

$$\frac{dP}{dx} = -\left(\frac{\eta}{K_v}\right) v - \left(\frac{\rho}{K_i}\right) v^2 \qquad (6)$$

where ρ is the density of the fluid in kg/m^3 and K_i is the inertial permeability in m. Because of the pressure dependence of the density, for through-plane measurements with constant velocity integration of (6) leads to:

$$\frac{P_{in}^2 - P_{out}^2}{2LP_0} = \frac{P_{in}^2 - P_0^2}{2LP_0} = \left(\frac{\eta}{K_v}\right) v_0 + \left(\frac{\rho_0}{K_i}\right) v_0^2 \qquad (7)$$

For in-plane transport, the spatial coordinate is radius r, so that the Darcy-Forchheimer equation has to be integrated between R_i to R_e. The overall pressure gradient in the porous material volume is then expressed as:

$$\frac{P_{in}^2 - P_0^2}{2(R_e - R_i)P_0} = \left(\frac{\eta}{K_v}\right) v_{av,0} + \left(\frac{\rho_0}{K_i}\right) v_{av,0}^2 \frac{(R_e - R_i)^2}{R_i R_e Ln\left(R_e / R_i\right)} \qquad (8)$$

For experiments with the fuel cell, velocity v_0 related to postulated through-plane transport in the GDL was calculated at T, P_0, on the basis of the channel area of the flow pattern. Treatment of the data using Eqn. 4 or 7 led to an estimate of the equivalent permeability of the GDL in the fuel cell design investigated. The equivalent permeability value can be used for comparison purposes of the GDL type or BP flow pattern.

For all data, the compressible pressure gradient was plotted versus velocity v_0 or $v_{av,0}$: in the latter case only for in-plane transport in the fundamental cell. The gas viscosity, which is temperature-dependent was determined by using Sutherland's viscosity law. The density of the gas was found using the perfect gas law.

Additionally, an attempt in estimating the permeability of the MPL was carried out. For this purpose, BC grade GDLs were assumed to consist of the corresponding BA substrate and the MPL deposited, neglecting the existing penetration of small carbon particles and hydrophobic resins in the external part of the substrate, caused by the elevated pressure and temperature during the manufacturing process. Depending on the configuration (through-plane or in-plane transport), the equations to be written differ largely from each other as illustrated in Fig. 3:

(i) For through-plane transport, the gas has to percolate successively through the MPS, then through the MPL; in this case, neglecting the different porosity of the two sub-layers, the velocity in the porous medium is the same, and the overall pressure drop is the sum of two pressure drops ; $\Delta P_{GDL} = \Delta P_{MPS} + \Delta P_{MPL}$. From the data obtained with BA- and BC-type GDL, the pressure drop of the gas flow through the MPL could be calculated for each v_0 value. Eqn. 4 was then applied to the MPL, with the rearrangement as follows:

$$\frac{P_{in,MPL}^2 - P_{out,MPL}^2}{2L_{MPL}\,P_0} = \frac{\Delta P_{MPL}\,P_{av,MPL}}{LP_0} = \left(\frac{\eta}{K_{v,MPL}}\right).v_0 \qquad (9)$$

where subscript MPL is for this sub-layer. The average pressure in the MPL, $P_{av,MPL}$ has been approximated as the average pressure of the gas in the whole GDL at the same gas velocity, making it possible to estimate $K_{v,MPL}$. The "subtraction" method had formerly been reported [15,24] but by neglecting the pressure gradient in the GDL, yielding an analytical expression for the MPL permeability, which was not used here.

(ii) For in-plane transport, the gas is distributed in the two layers, with the same pressure drop, and the local velocities in the two layers depend on compared permeability values, in relation to the overall permeability of the BC grade investigated. Two equations for the expression of the pressure difference across each layer can be established versus the corresponding viscous permeability using Eqn. 5. The above two-equation set was solved numerically.

4. Results and discussion

The experimental results obtained for the through-plane and the in-plane permeability of the GDLs used in the different cells are discussed here.

4.1. The through-plane permeability in the fundamental cell

In through-plane configuration, the pressure drop measured in the fundamental cell was shown to vary linearly with the applied flow rate, which results in a linear dependence of the pressure gradient on the average velocity (Figures 4a and b), expressing laminar flow. The through-plane permeability values of the selected GDLs were then determined by fitting the experimental data to Darcy's law (Eqn. 4). The experimental results and the curve fitting are shown in Figure 4 a and b and the obtained values for the permeability are given in Table 3.

The average through-plane permeability of GDL 24 BC comprising the substrate and the MPL was found at 6.0 x 10^{-14} m^2. The obtained value is in agreement with the reported value for this GDL at 1.46 x 10^{-13} m^2 and 5.96 x 10^{-14} m^2 [9]. Similarly, for the through-plane permeability, the value determined for SGL 24 BA was on an average at 5.8 x 10^{-12} m^2, which is somewhat lower than the published value at 1.47 x 10^{-11} m^2 in ref. [2]. For the equivalent MPS without PTFE impregnation (24 AA), the permeability was found slightly lower at 5.2 x 10^{-12} m^2. The permeability difference between 24 BA and 24 AA might be explained by the fact that AA structure not protected by PTFE, thus would be more prone to compression when clamped in the cell. The permeability for 28 AA was shown to be somewhat larger than that of 24 AA (Table 3).

For GDL 34 BA, the average through-plane permeability was determined at 3.3 x 10^{-11} m^2; the uncertainty was estimated at 20% due to the very low-pressure differences, in spite of the more accurate sensor used. This value is in acceptable agreement with the available literature value of (1.63, 1.88 and 2.74) x 10^{-11} m^2 reported in [2,9]. However, the obtained value is far larger than that of 24 BA, as confirmed by replicate experiments (Figure 4a): this might be caused by the more widely dispersed morphology of the fibers (data not shown).

For the GDL 34 BC, the overall through-plane permeability value was found on an average at 1.1 x 10^{-13} m^2 : the large deviation from the formerly published (Table 3) could not be explained up to now. The permeability value is approx. two times larger than 24 BC grade, which may be the fact of very different behaviour of their MPS. Permeability of more recent grades 28 BC and 38 BC were found larger than 2 x 10^{-13} m^{-2}.

For BC-grade GDLs, the permeability was found to be nearly two orders of magnitude below than that in AA- or BA- grade materials. Because the sub-layers are percolated in series by the gas (Figure 3), the pressure drop in BC grade GDLs is mainly due to the MPL, with a nearly negligible contribution of the MPS.

4.2. The in-plane permeability in the fundamental fuel cell

Limited work has been done to measure the in-plane permeability for GDLs, and not much literature was found to acknowledge the range of the obtained values. Manufacturers usually specify the GDLs with an approximate range of air permeability values, often without mention on through-plane or in-plane transport.

Because of the aforementioned linear variation of the pressure gradient with the average gas velocity calculated with Eqn. 2 (Figure 5a and b), the data have been also fitted to Darcy's law (Eqn. 5) for estimation of in-plane permeability. The values obtained are gathered in Table 3. The in-plane permeability determined for GDL 24 BA was 9.9 x 10^{-12} m^2. For GDL 24 AA without PTFE, the average in-plane permeability was found at 7.2 x 10^{-12} m^2, with the likely same reason as for through-plane transport. The permeability value exhibited by GDL 34 BA and 28 AA were found to be quite larger than those of the two first GDLs, as observed above for through-plane gas transport. For the GDL 34 BC, the average in-plane permeability value was found at 4.6 x 10^{-12} m^2. This value is also 60% larger than the permeability in 24 BC - 2.7 x 10^{-12} m^2 - and the reasons given in section 4.1 could also be invoked here. In addition, in-plane permeability of grades 28 and 38 BC are approx. two times larger than of 34 BC GDL.

The presence of the MPL appears to have a lesser impact on the permeability for in-plane transport, with a ratio (BA grade/BC grade) lower than 10. Here, as explained above, the flow is distributed radially in the two sub-layers and because of the very different pore size distributions and permeability of MPS and MPL, the gas flows principally in the MPS layer, so that the overall pressure drop in the 24 BC and 34 BC is to be comparable to that in the corresponding MPS layer. Besides, the through-plane (TP) over in-plane permeability (IP) ratio is shown to vary from 0.50 to 0.94 for macroporous substrates, and only in the range 0.022-0.033 for MPL-containing GDLs: for the first GDL group without MPL, this ratio highlights the equivalent ease with which molecules flow in both directions (TP and IP) independently. For the second GDL group (with GDL), the obtained low ratio is the fact of a very low TP permeability, the MPL acts as a barrier making TP transport difficult in this layer, then fostering the IP transport in the MPS.

4.3. The permeability values obtained for MPL

Permeability values for MPL of 24 BC, 34 BC and 28 BC samples, $K_{v,MPL}$, were estimated using Eqn. 9: with 28 BC grade, the permeability of the 28 AA grade has been used, neglecting the effect of the PTFE charge in the MPS. The equivalent TP permeability of the

MPL was found at 1.04, 1.40 and 4.65 x 10^{-14} m^2 for GDL types 24, 34 and 28 respectively. The visible difference between 24-34 and 28 types, might be due to different MPL nature and deposition process at high temperature and pressure. Estimate for the MPL contained in 34 BC and found in the literature was reported at 13.5 x 10^{-14} m^2 [9], nearly one order of magnitude larger than that obtained here. Numerical simulations using Eqn. 9 shows that changing K_v value of the MPS by 10% affects the MPL permeability value by less than 1%, whereas a 10% change in $K_{v,GDL}$ results in an equivalent change in $K_{v,MPL}$, because of the very different orders of magnitude of the permeability of MPS and MPL.

For the case of in-plane permeability, the separate values for K_v with related BA and BC ; GDL did not lead to realistic values for the MPL permeability (data not shown). This can be easily explained by the fact that the two sublayers are far from independent from each other due to the MPL deposition protocol involving high-pressure deposition and thermal annealing, resulting in the existence of the "penetration" layer: this intermediate area likely acts as an additional barrier to the gas flow, thus affecting the gas transport in the heterogeneous structures of the GDL. This comment also holds for through-plane measurements, indicating the only moderate confidence one can have in $K_{v,MPL}$ estimates.

4.4. Equivalent permeability values obtained with the two bipolar plates for fuel cells

In a general manner, the pressure drop between the GDL sample stacked between two bipolar plates varied between 6 to 50 mbars for the largest flow rate, whatever the GDL structure. The compressible pressure gradients were actually in the order of 2 - 4 x 10^6 Pa/m for grades AA and BA, and from 6 to 14 x10^6 Pa/m with BC grade GDLs. As exemplified in Figure 6 for the case of multiple channel flow pattern, the compressible pressure gradient through the GDL stacked between the two bipolar plates does not vary linearly with gas velocity v_0, calculated on the basis of the channel area. The deviation from Darcy's law actually appears for velocity larger than a few mm/s, regardless of the presence of an MPL. Therefore, Darcy-Forchheimer was used, considering through-plane transport (Eqn. 7), as explained in Section 3.2, for estimation of equivalent viscous and inertial permeability in the fuel cell. The obtained values are reported in Table 4 for the eight GDLs investigated. Moreover, contrary to what was observed for through-plane transport in the fundamental cell (section 4.1), pressure gradients with BC type GDLs were not orders of magnitude larger than those with AA or BA type layers (Figure 6).

The pressure gradient observed in the single-channel flow pattern is 15-30% higher than in multiple channel configuration. As a consequence, lower equivalent permeability values were obtained with single serpentine than with multiple ones (Table 4).

- *Importance of inertial flow contribution*

Comparing the equivalent viscous and inertial permeability respectively for the two BP sets has to be considered with caution, nevertheless comparing the contribution of the inertial pressure gradient with reference to the overall pressure gradient can be proposed. For this purpose, the permeability estimates obtained in the cell make it possible to estimate the significance of inertial flow for 1 A/cm^2, X_i, in the pressure drop in the porous structure, as follows:

$$X_i = \frac{\left(\frac{\rho_0}{K_i}\right) v^2_{0,i=1A/cm^2}}{\left(\frac{\eta}{K_v}\right) v_{0,i=1A/cm^2} + \left(\frac{\rho_0}{K_i}\right) v^2_{0,i=1A/cm^2}} \qquad (10)$$

The X_i values obtained are in the order of 0.3 - 0.4 for MPL-free GDLs, and below 0.17 with BC grade GDLs (Figure 7). In comparison with what was observed with the fundamental cell, the inertial flow in the GDL even at lower velocity appears far more significant. The effect of the flow pattern is not significant for AA and BA type GDLs, whereas, with the presence of an MPL, X_i ranges within 0.10- 0.14 in single-serpentine configuration, and from 0.13 to 0.17 with multiple channel flow pattern.

The difference in flow regime between the fundamental cell and the FC bipolar plates is at least to a part due to the gas flow direction upstream of the GDL surface.

- As a matter of fact, in the fundamental cell, the gas arrives perpendicular to the GDL surface area for both TP or IP configurations: the flow is forced to cross the porous structure without random-like motion. The gas flow can be considered as guided and ordered as in laminar flow across the GDL, with pressure gradients obeying Darcy's law.
- With the GDL stacked between the BPs, the gas arrives tangential to the porous structure, then either flowing further in the channel or changing direction to flow across the GDL. Moreover in the stacked GDL, the gas can flow either through-plane or in-plane as in by-passing flow. The observed inertial contribution in the pressure gradients in the stacked GDL appears consistent with that in former works [20,22,23] which evidenced the fact

that the pressure drop between two adjacent channels was no linear relation of the under-land flow rate.

Nevertheless, it can be observed in Figure 7 that the inertial contribution is lower for the BC-group GDLs than for the AA- and BA- group. Indeed for the first group, the presence of the MPL acting as additional resistance to TP transport, can result in more ordered flow by favoring part of the gas to flow along the MPL in IP flow in the MPS. This is to result in inertial contribution decrease in comparison to that in MPL-free GDLs.

Now, except for AA-type GDLs, the significance criterion for the inertial term, X_i, is on average 30% lower with a single serpentine flow pattern than with multiple serpentine. This flow rate corresponds to average velocity v_0 with a single serpentine flow pattern approx. 23% larger than with the other: the larger velocity might better guide the gas flow through the GDL, thereafter limiting the inertial contribution. AA-type GDLs are more prone to local compression and disorganization of its structure due to PTFE absence. Because the rib area of the bipolar plate with single serpentine is larger than with multiple serpentine; therefore higher compression on the GDL could be expected with single serpentine, thus resulting in higher flow disorder and higher inertial contribution (Figure 7).

- *Comments on equivalent permeability in a stacked GDL*

One significant fact mentioned above is that the presence of an MPL in the GDL reduces the equivalent viscous permeability by a factor of 3 or 4, far lower than the factor 30- or 100 ~~factor~~ obtained in the fundamental cell for through-plane permeability (see above). By contrast, this factor was found to be more consistent with its corresponding value for in-plane permeability, reported above to vary from 2 to 7: as for in-plane flow, and because the gas is fed tangentially to the GDL, the presence of an MPL does not affect dramatically to the equivalent permeability: this may also indicate on the occurrence of channel by-passing. These comments hold for both flow patterns.

On an average, the data reported in Table 4 show that the equivalent viscous permeability of a macroporous substrate (AA or BA type) in the cell with single- or multiple serpentine channels, is 15 to 100 times lower than that of through-plane and in-plane permeability (Table 3): this fact was observed with all macroporous substrates samples tested, is likely attributable to the orientation of the gas flow upstream of the GDL, being perpendicular to the GDL surface in the dedicated cell, and parallel when using the bipolar plates.

4.5 The effect of permeability on fuel cell performance

The cell performance in terms of the voltage vs. current density variations is significantly affected by the nature of the GDL (Figure 8). The cell voltage measured at 0.8 A/cm^2 with GDL 28 BC and 38 BC is approx. 210 mV larger than that with 24 BC and 34 BC, 38 BC grade allowing the best performance. The performance of the fuel cell obeys the relationship: 38 BC > 28 BC > 34 BC > 24 BC, in agreement with the viscous permeability value measured when the GDL was stacked between the multiple-channel BP's (Table 4). The far larger performance allowed by 28 and 38 BC might originate from more efficient MPL technology. Moreover, the sudden drop in cell voltage due to concentration loss starts from 0.85 A/cm^2 current density in 38 BC, whereas, the drop is seen at 0.7 A/cm^2 onwards for 24 BC. Clearly, diversity in MPL strata is evident in these GDLs, as gas permeability across these GDLs stacked between the BPs are linked to losses associated with mass transfer: enhanced gas transport would lead to higher cell potential and power density.

5. Conclusion

In this work, the through-plane and in-plane permeabilities across selected GDLs with and without MPL coating have been measured using an in-house designed fundamental cell. Over a broad range of gas velocity through the porous layers, the pressure measured was found to obey Darcy's law. For macroporous substrates GDL, through-plane and in-plane permeability although different, are in the same order of magnitude, whereas the flow direction has a strong effect on the permeability for MPL-comprising GDLs. Differential analysis of the behavior of two GDLs having the same substrate, in the hope of estimating the contribution of the MPL, was shown to be moderately rigorous, because of its appreciable penetration in the macroporous substrate. Besides, gas flow behavior through a GDL stacked in a fuel cell was shown to largely differ from that in the fundamental cell, in particular by the higher significance of inertial flow in the transport, depending on the flow pattern. Equivalent permeability estimated in a fuel cell, which likely covers the occurrence of combined through-plane and in-plane transport with local compression of the MPS at the channel edges, was observed to strongly differ from the values obtained in the dedicated fundamental cell, for all GDLs tested. These equivalent values should be used as in modeling investigations of fuel cell operations, instead of in-plane or through-plane permeability obtained in a dedicated cell. Moreover, upon using MPL loaded GDLs, and putting it to test under real working conditions,

the fuel cell performance curves are consistent with the effective permeability in relation to concentration losses. In view to modeling operation of PEM fuel cell of a given flow pattern, the equivalent permeability K_v could be estimated using the method proposed here, on the basis of postulated through-plane transport, with average velocity v_0 referred to the channel area $S_{channel}$.

Nevertheless, the approach needs to be refined for better representation of the various transport phenomena in a FC under operation, e.g. diffusion through the GDL and larger flow velocity in the channel, for air usually fed with a large excess. Moreover, an understanding is currently developed in finding out the influence of cell plate design on the overall transport. For the first point, the distribution of pressures and stress applied to the GDL should be modeled or at least estimated. Secondly, local measurements of gas permeability of the GDL stacked between two bipolar plates would indicate on transport rate distribution over the MEA area. Also, usage of mixed gases, humidified gases, and the presence of water droplets are proposed to be tested, to better emulate flow phenomena in GDL in real operating conditions in a fuel cell.

Acknowledgments

The authors would like to extend their gratitude to Université de Lorraine for financial assistance provided as a Ph.D. grant for Mainak Mukherjee. The authors also thank the mechanical workshop of the lab for his significant contribution in the cell design and construction.

References

[1] Lapicque F, Belhadj M, Bonnet C, Pauchet J, Thomas Y. A critical review on gas diffusion micro and macroporous layers degradations for improved membrane fuel cell durability. J.Power Sources 2016; 336: 40–53. https://doi.org/10.1016/j.jpowsour.2016.10.037

[2] Gostick J.T, Fowler M.W, Pritzker M.D, Ioannidis M.A, Behra L.M. In-plane and through-plane gas permeability of carbon fiber electrode backing layers. J. Power Sources 2006 ; 162 : 228–238. https://doi.org/10.1016/j.jpowsour.2006.06.096

[3] Bessler W.G, Gewies S, Vogler M. A new framework for physically based modeling of solid oxide fuel cells. Electrochim. Acta 2007; 53 : 1782–1800. https://doi.org/10.1016/j.electacta.2007.08.030

[4] Ismail M.S, Borman D, Damjanovic T, Ingham D.B, Pourkashanian M. On the through-plane permeability of microporous layer-coated gas diffusion layers used in proton exchange membrane fuel cells. Int.J. Hydrog. Energ 2011; 36: 10392-10402. https://doi.org/10.1016/j.ijhydene.2010.09.012

[5] El-Kharouf A, Mason T.J, Brett D.J.L, Pollet B.G. Ex-situ characterisation of gas diffusion layers for proton exchange membrane fuel cells. J. Power Sources 2012; 218 : 393–404. https://doi.org/10.1016/j.jpowsour.2012.06.099

[6] Ge J, Higier A, Liu H. Effect of gas diffusion layer compression on PEM fuel cell performance. J. Power Sources 2006 ; 159 : 922–927. https://doi.org/10.1016/j.jpowsour.2005.11.069

[7] Park S, Lee J.W, Popov B.N. A review of gas diffusion layer in PEM fuel cells: Materials and designs. Int. J. Hydrog. Energ. 2012; 37 : 5850–5865. https://doi.org/10.1016/j.ijhydene.2011.12.148

[8] Cindrella L, Kannan A.M, Lin J.F, Saminathan K, Ho Y, Lin C.W, Wertz J. Gas diffusion layer for proton exchange membrane fuel cells-A review. J. Power Sources 2009; 194:146–160. https://doi.org/10.1016/j.jpowsour.2009.04.005

[9] Pant L.M, Mitra S.K, Secanell M. Absolute permeability and Knudsen diffusivity measurements in PEMFC gas diffusion layers and micro porous layers. J. Power Sources 2012 ; 206 : 153–160. https://doi.org/10.1016/j.jpowsour.2012.01.099

[10] Mangal P, Pant L.M, Carrigy N, Dumontier M, Zingan V, Mitra S, Secanell M. Experimental study of mass transport in PEMFCs: Through-plane permeability and molecular diffusivity in GDLs. Electrochim. Acta 2015;167 : 160–171. https://doi.org/10.1016/j.electacta.2015.03.100

[11] Prasanna M, Ha H.Y, Cho E.A, Hong S.A, Oh I.H. Influence of cathode gas diffusion media on the performance of the PEMFCs. J. Power Sources 2004; 131 : 147–154. https://doi.org/10.1016/j.jpowsour.2004.01.030

[12] Tamayol A, Bahrami M. Water permeation through gas diffusion layers of proton exchange membrane fuel cells. J. Power Sources 2011 ; 196 : 6356–6361. https://doi.org/10.1016/j.jpowsour.2011.02.069

[13] Feser J.P, Prasad A.K, Advani S.G. Experimental characterization of in-plane permeability of gas diffusion layers. J. Power Sources 2006 ; 162 : 1226–1231. https://doi.org/10.1016/j.jpowsour.2006.07.058

[14] Tranter T.G, Stogornyuk P, Gostick J.T, Burns A.D, Cale W.F. A method for measuring relative in-plane diffusivity of thin and partially saturate porous media: an application to fuel cell gas diffusion layers. Int. J. Heat Mass Transfer 2017 ; 110 : 132-141. https://doi.org/10.1016/j.ijheatmasstransfer.2017.02.096

[15] Zhiani M, Kamali S, Majidi S. In-plane gas permeability and through-plane resistivity of the gas diffusion layer influenced by homogenization technique and its effect on the proton exchange membrane fuel cell cathode performance. Int. J. Hydrog. Energ. 2016 ; 41 : 1112-1119. https://doi.org/10.1016/j.ijhydene.2015.10.052

[16] Radhakrishnan V, Haridoss P. Effect of cyclic compression on structure and properties of a Gas Diffusion Layer used in PEM fuel cells. Int. J. Hydrog. Energ. 2010 ; 35 : 11107–11118. https://doi.org/10.1016/j.ijhydene.2010.07.009

[17] Orogbemi O.M, Ingham D.B, Ismail M.S, Hughes K.J, Ma L, Pourkashanian M. Through-plane gas permeability of gas diffusion layers and microporous layer: Effects of carbon loading and sintering. J. Energy Inst 2018; 91 : 270–278. https://doi.org/10.1016/j.joei.2016.11.008

[18] Schmittinger W, Vahidi A. A review of the main parameters influencing long-term performance and durability of PEM fuel cells. J. Power Sources. 2008 ; 180 : 1–14. https://doi.org/10.1016/j.jpowsour.2008.01.070

[19] Pharoah J.G. On the permeability of gas diffusion media used in PEM fuel cells. J. Power Sources 2005 ; 144 :77-82. https://doi.org/10.1016/j.jpowsour.2004.11.069

[20] Feser J.P, Prasad A.K, Advani S.G. On the relative influence of convection in serpentine flow fields of PEM fuel cells. J. Power Sources 2006 ;161 : 404-412. https://doi.org/10.1016/j.jpowsour.2006.04.129

[21] Park J, Li X. An analytical analysis on the cross flow in a PEM fuel cell with serpentine flow channel. Int. J. Energy Res. 2011 ; 35 : 583-593. https://doi.org/10.1002/er.1712

[22] Zhang XY, Zhang X, Taira H, Liu H. Errors of Darcy's law for serpentine flow fields: an analytical approach. Int. J. Hydrog. Energ. 2018; 43 : 6686-6695. https://doi.org/10.1016/j.ijhydene.2018.02.070

[23] Taira H, Liu H. In-situ measurements of GDL effective permeability and under-land cross-flow in a PEM fuel cell. Int. J. Hydrog. Energy 2012 ; 37 : 13725-13730. https://doi.org/10.1016/j.ijhydene.2012.03.030

[24] Gurau V, Bluemle M.J, Castro De E.S, Tsou Y.M, Zawodzinski T.A, Mann J.A. Characterization of transport properties in gas diffusion layers for proton exchange membrane fuel cells 2. Absolute permeability. J. Power Sources 2007 ; 165 (2):793-802. https://doi.org/10.1016/j.jpowsour.2006.12.068

Table 1. Comparative chart of the different configurations of cells used.

Parameters	**Fundamental Cell**	**Single Channel**	**Multiple Channel**
Tested GDL	All	All	All
Size of GDL	A circular disc of diameter; 20 mm	Square piece 5.3 x 5.3 cm^2	Square piece 5.3 x 5.3 cm^2
Active surface area considered (cm^2)	-Through-plane: 0.196 (⌀ 5 mm) -Radial flow in in-plane configuration	(Channel area) 13.1	(Channel area) 16.2
Flowrate (NmL/min)	10-150	100-1000	100-1000
Used for	Through-plane and in-plane individually	Equivalent permeability	Equivalent permeability

Table 2. Selected GDLs from Sigracet Germany used for the permeability measurements. MPS was a carbon paper in all GDLs.

GDL (SGL Carbon)	Thickness	Basic weight (g/m^2)	Porosity	PTFE treated MPS	MPL
24 AA	190 ± 10	52.4	0.85	No	No
24 BA	200 ± 10	55	0.82	Yes (5%)	No
28 AA	230 ± 10	100	0.76	No	No
34 BA	270 ± 10	78.7	0.83	Yes (5%)	No
24 BC	230 ± 10	100	0.76	Yes	Yes
28 BC	240 ± 10	105	0.76	Yes	Yes
34 BC	320 ± 10	126	0.75	Yes	Yes
38 BC	320 ± 10	125	0.77	Yes	Yes

Table 3. Through-plane and in-plane viscous permeability in the fundamental cell

GDL (SGL Carbon)	Through-plane (Fundamental cell) m^2 ± 10%	In-plane (Fundamental cell) m^2 ± 10%	Literature Value (Through-plane) m^2
24 AA	5.1×10^{-12}	7.2×10^{-12}	-
24 BA	5.8×10^{-12}	9.9×10^{-12}	$(6.5 - 14.5) \times 10^{-12}$ [2] Air
28 AA	8.1×10^{-12}	1.6×10^{-11}	-
34 BA	3.3×10^{-11}	3.5×10^{-11}	$(1.6 – 2.7) \times 10^{-11}$, [9] Nitrogen
24 BC	6.0×10^{-14}	2.7×10^{-12}	$(0.59, 1.46) \times 10^{-13}$ [9], Nitrogen
28 BC	2.7×10^{-13}	8.7×10^{-12}	-
34 BC	1.1×10^{-13}	4.6×10^{-12}	$4.4\text{-}7.9 \times 10^{-13}$ [9] Nitrogen
38 BC	2.9×10^{-13}	9.0×10^{-12}	-

Table 4 : Equivalent viscous and inertial permeability of the GDLs stacked between 25 cm^2 bipolar plates with the two flow patterns investigated.

GDL (SGL Carbon)	**Multiple channel**		**Single channel**	
	Eq. K_v (m^2)	Eq. K_i (m)	Eq. K_v (m^2)	Eq. K_i (m)
24 AA	1.85×10^{-13}	1.22×10^{-10}	1.50×10^{-13}	1.03×10^{-10}
24 BA	1.91×10^{-13}	1.04×10^{-10}	1.27×10^{-13}	2.12×10^{-10}
28 AA	2.09×10^{-13}	1.17×10^{-10}	1.58×10^{-13}	8.88×10^{-11}
34 BA	3.69×10^{-13}	1.51×10^{-10}	2.67×10^{-13}	1.66×10^{-10}
24 BC	6.12×10^{-14}	9.72×10^{-11}	4.41×10^{-14}	9.24×10^{-11}
28 BC	8.80×10^{-14}	2.40×10^{-10}	4.58×10^{-14}	1.09×10^{-10}
34 BC	7.51×10^{-14}	1.81×10^{-10}	4.49×10^{-14}	1.03×10^{-10}
38 BC	9.91×10^{-14}	3.61×10^{-10}	5.80×10^{-14}	1.11×10^{-10}

Legends of figures

Figure 1: The design and fabricated measurement 'fundamental' cell and bipolar plate designs of real 25 cm^2 fuel cells; (a-b) Design of dedicated cell, (c) After fabrication of dedicated cell.

Figure 2: View of the fuel cell, in operation (a) or used for permeability measurements (b), and with the approach considered here (c) with uniform velocity v_0.

Figure 3: Schematic analysis for the through-plane and in-plane transports in GDLs used here.

Figure 4: Through-plane compressible pressure gradient (Eqn. 4) vs. flow velocity v_0 at P_0 in (a) GDL without MPL; (b) in BC grade GDLs. Linear fittings of the data (Darcy's law) are in dotted lines.

Figure 5: In-plane compressible pressure gradient (Eqn. 5) vs. the average flow velocity, $v_{av,0}$, (c) in GDL without MPL; (d) in BC grade GDLs. Linear fittings of the data (Darcy's law) are in dotted lines.

Figure 6: Compressible pressure gradient through the GDL stacked between the bipolar plates (multiple serpentine channels) vs. the gas velocity v_0 calculated on the basis of through-plane transport over the channel area.

Figure 7: Fraction of the inertial contribution of pressure drop through the GDL for the two flow patterns and the eight GDLs tested.

Figure 8: Cell potential vs. current density 'polarisation curve' for MPL layered GDLs (24 BC, 34 BC, 28 BC, and 38 BC).

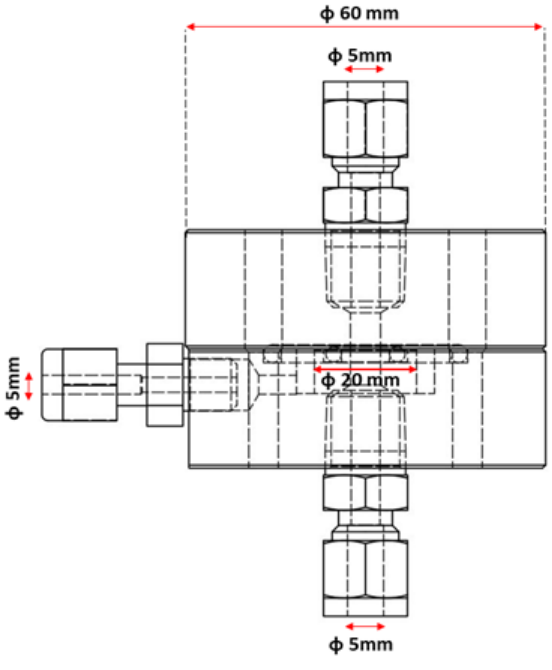

Assembly drawing

(a)

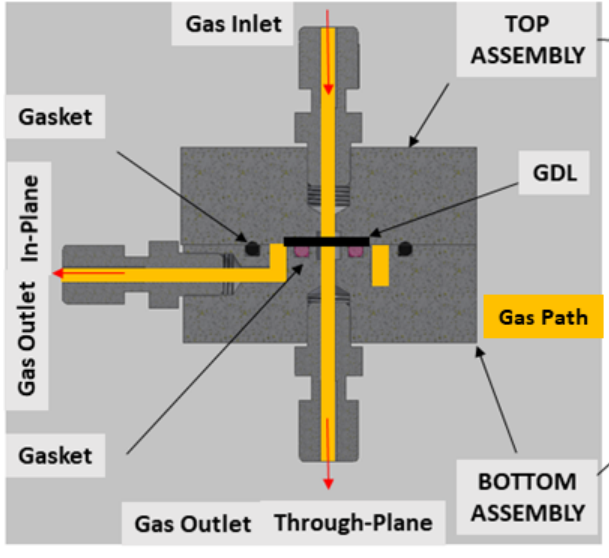

2-D image of the assembly

(b)

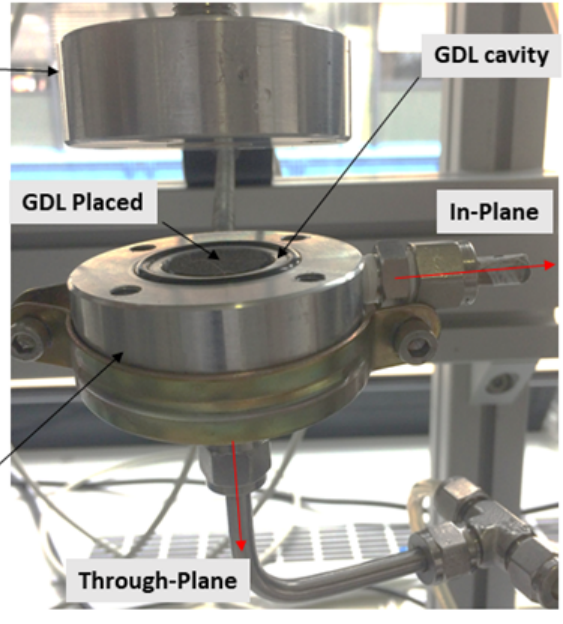

After fabrication

(c)

Figure 1

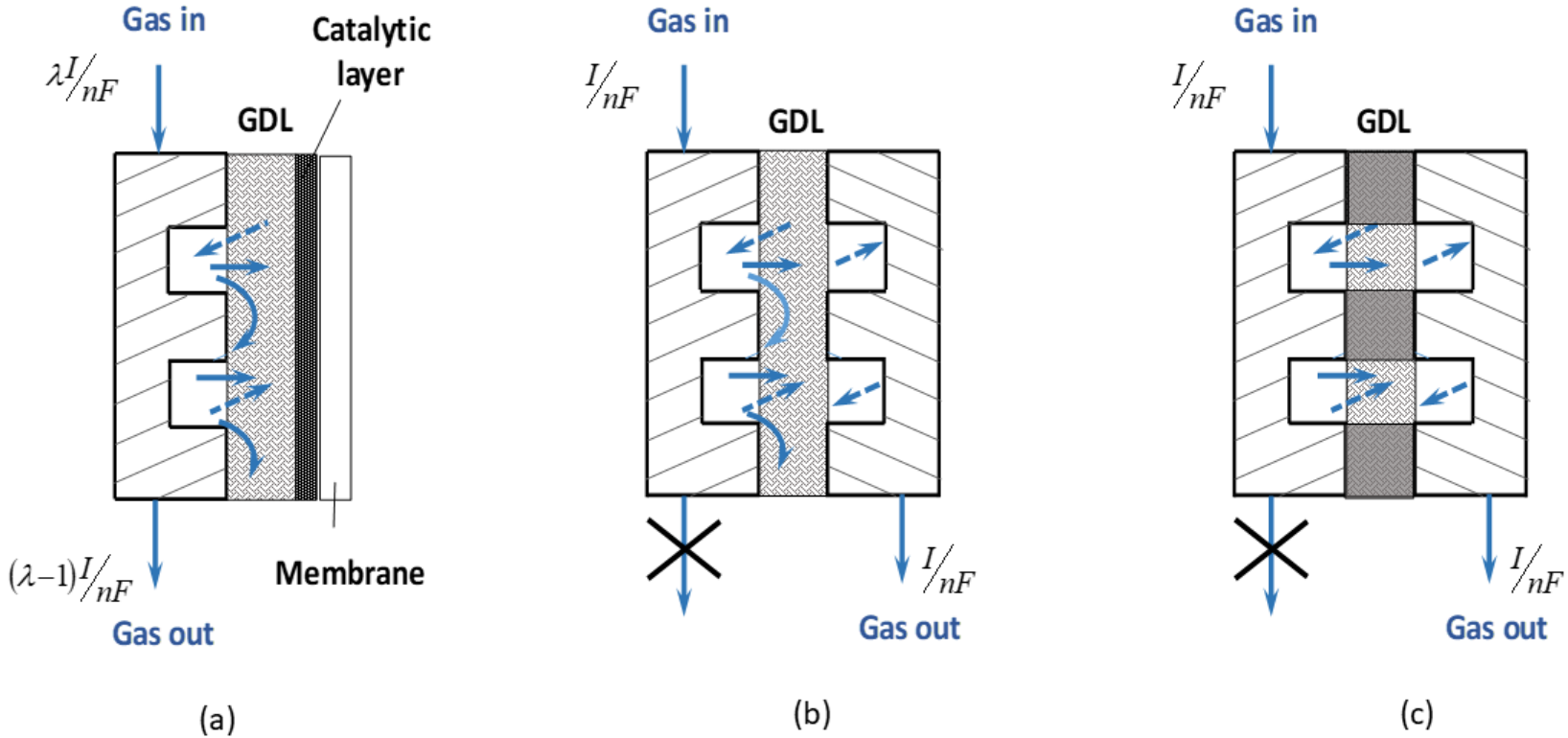
Gas in
Catalytic layer
$\lambda I/nF$
GDL
$(\lambda-1)I/nF$
Membrane
Gas out
(a)
Gas in
I/nF
GDL
I/nF
Gas out
(b)
Gas in
I/nF
GDL
I/nF
Gas out
(c)

Figure 2

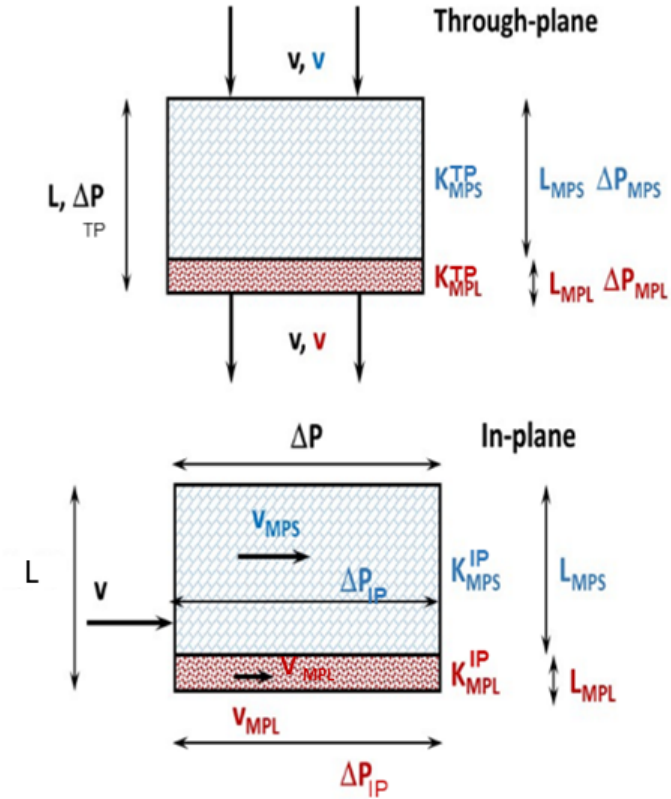
Through-plane
v, v
L, ΔP
TP
K^{TP}_{MPS}
K^{TP}_{MPL}
L_{MPS} ΔP_{MPS}
L_{MPL} ΔP_{MPL}
v, v
ΔP
In-plane
L
v
V_{MPS}
ΔP_{IP}
K^{IP}_{MPS}
K^{IP}_{MPL}
L_{MPS}
L_{MPL}
V_{MPL}
V_{MPL}
ΔP_{IP}

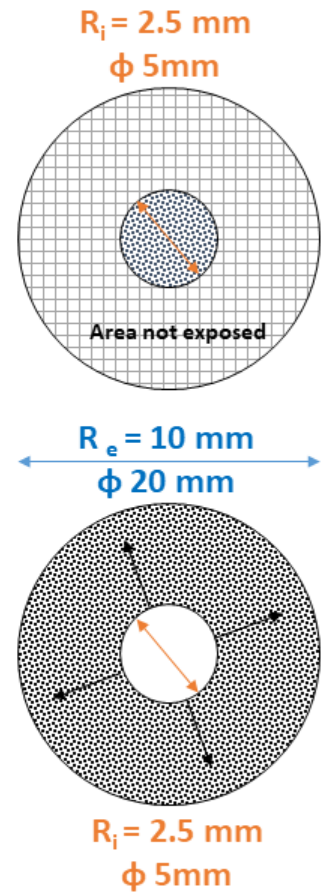
R_i = 2.5 mm
ϕ 5mm
Area not exposed
R_e = 10 mm
ϕ 20 mm
R_i = 2.5 mm
ϕ 5mm

Figure 3

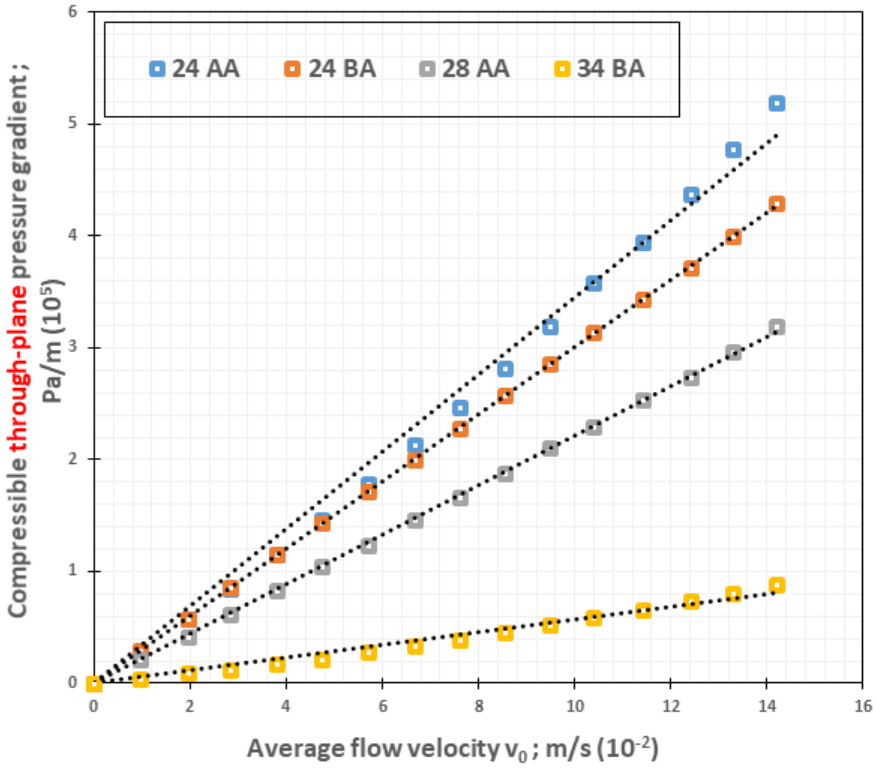
24 AA
24 BA
28 AA
34 BA
Compressible through-plane pressure gradient ; Pa/m (10⁵)
Average flow velocity v0 ; m/s (10-2)

(a)

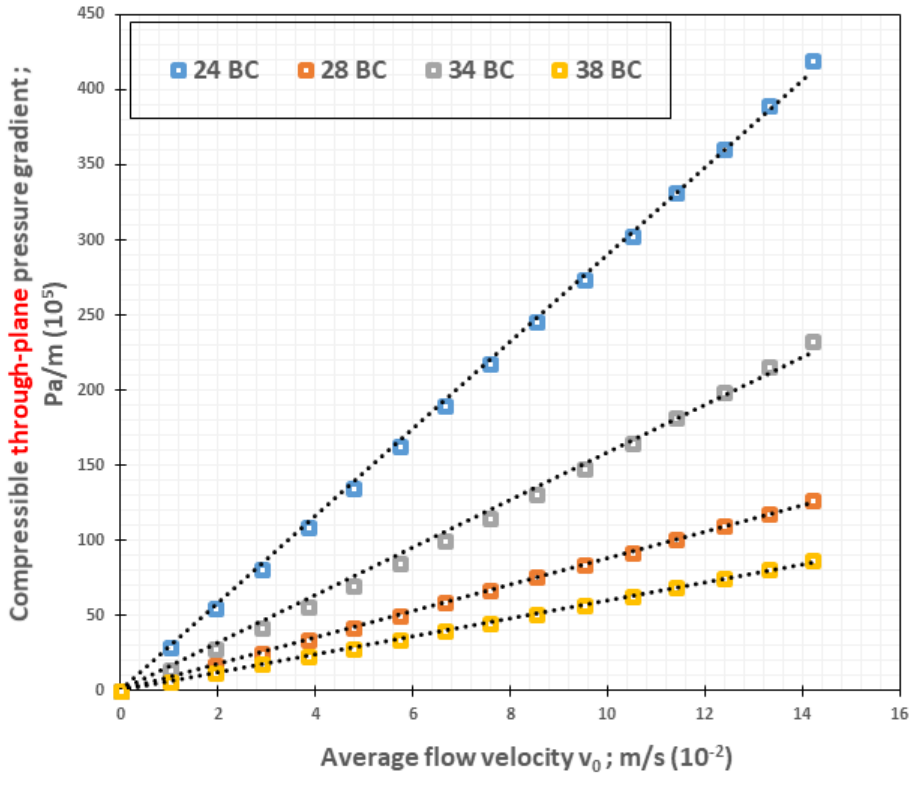
24 BC
28 BC
34 BC
38 BC
Compressible through-plane pressure gradient ; Pa/m (10⁵)
Average flow velocity v0 ; m/s (10-2)

(b)

Figure 4

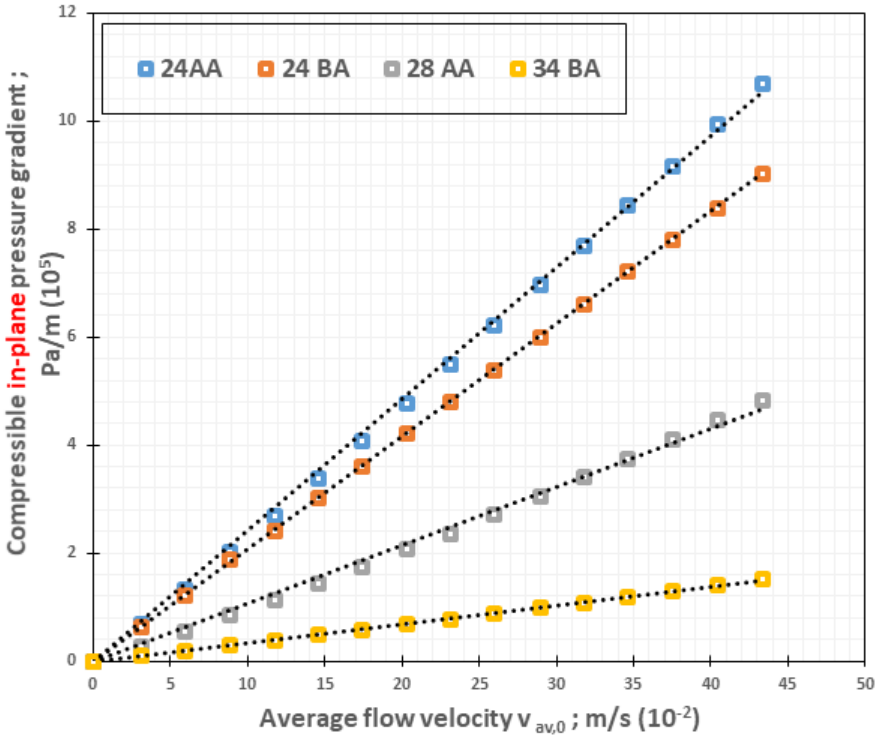
24AA
24 BA
28 AA
34 BA
Compressible in-plane pressure gradient ; Pa/m (10^5)
Average flow velocity v av,0 ; m/s (10^-2)
0
2
4
6
8
10
12
0
5
10
15
20
25
30
35
40
45
50

(a)

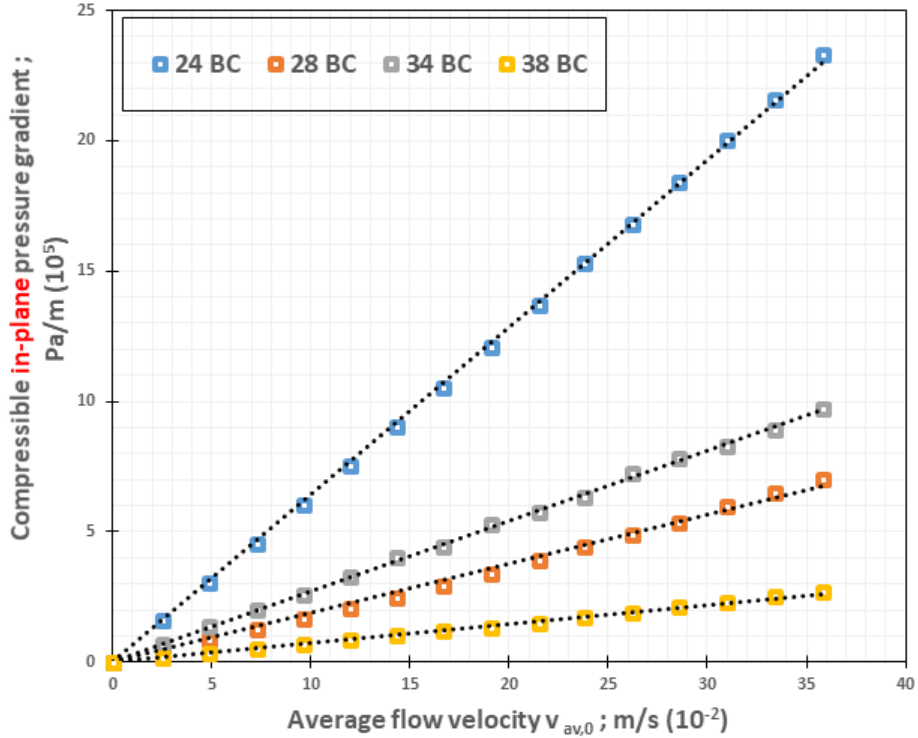
24 BC
28 BC
34 BC
38 BC
Compressible in-plane pressure gradient ; Pa/m (10^5)
Average flow velocity v av,0 ; m/s (10^-2)
0
5
10
15
20
25
0
5
10
15
20
25
30
35
40

(b)

Figure 5

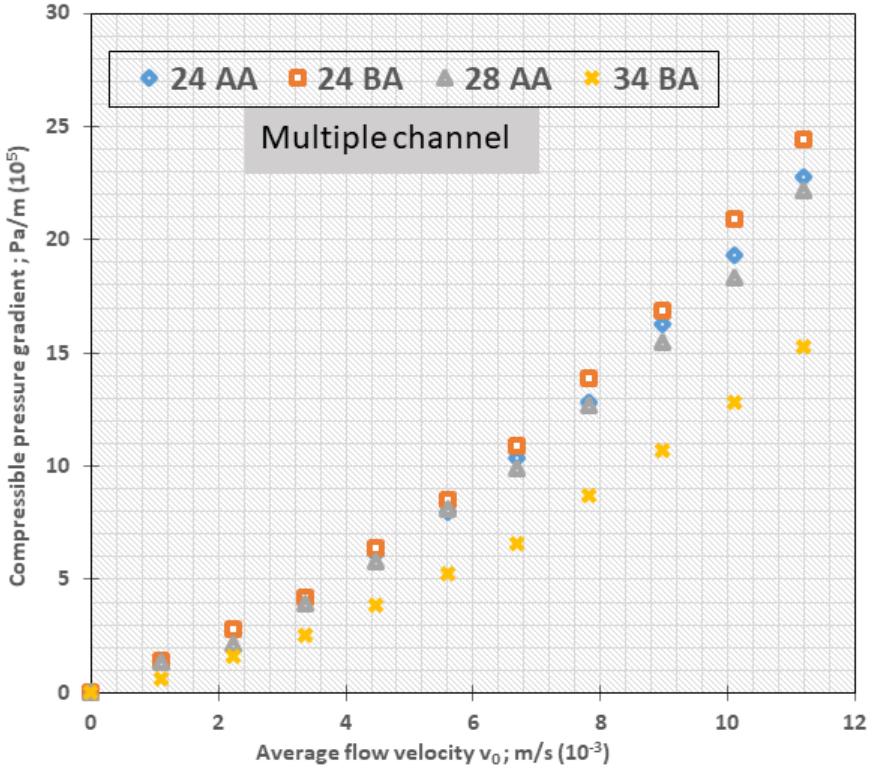
24 AA
24 BA
28 AA
34 BA
Multiple channel
Compressible pressure gradient ; Pa/m (10^5)
Average flow velocity v0 ; m/s (10^-3)
0
5
10
15
20
25
30
0
2
4
6
8
10
12

(a)

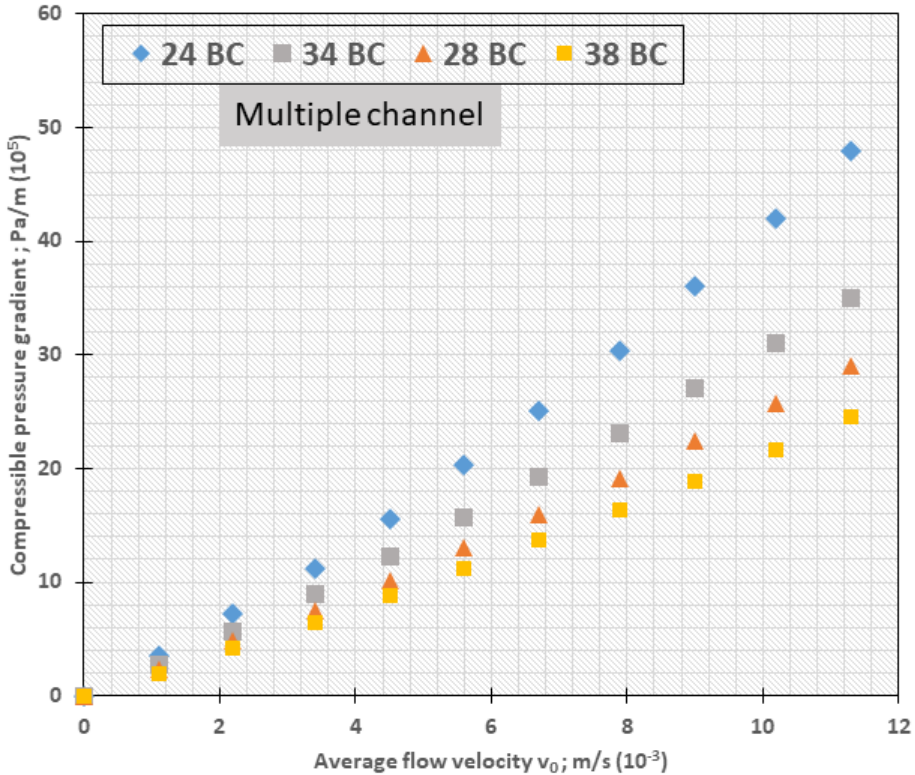
24 BC
34 BC
28 BC
38 BC
Multiple channel
Compressible pressure gradient ; Pa/m (10^5)
Average flow velocity v0 ; m/s (10^-3)
0
10
20
30
40
50
60
0
2
4
6
8
10
12

(b)

Figure 6

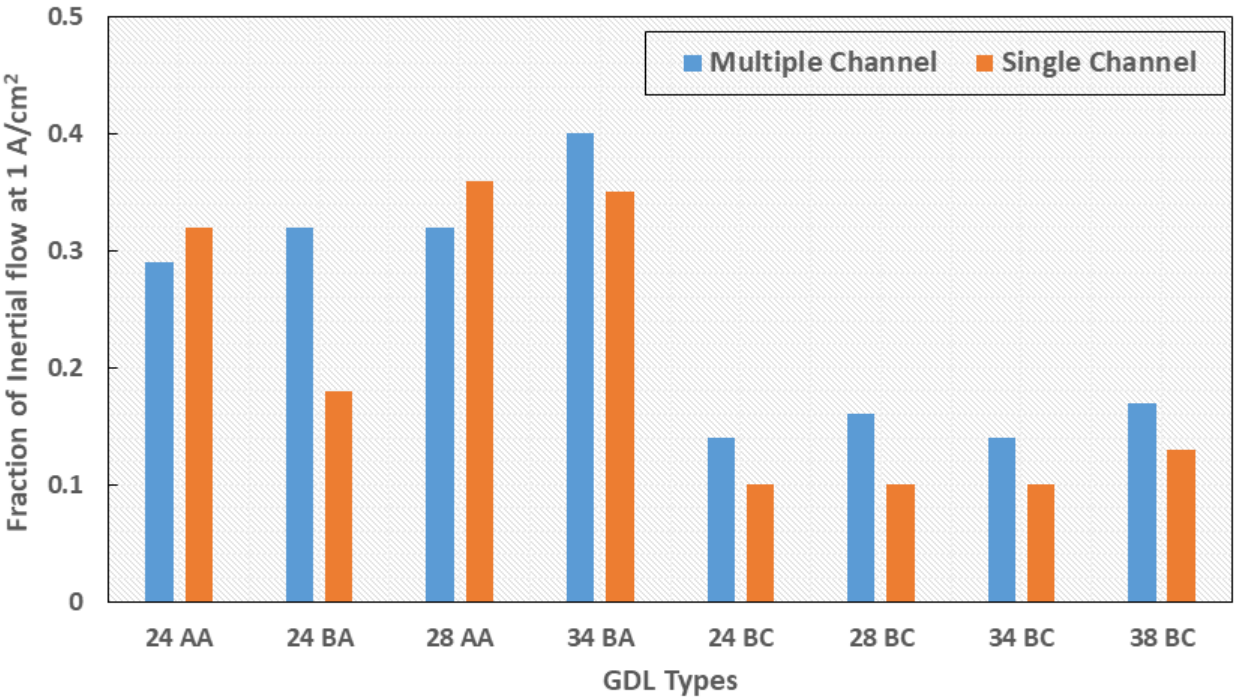
Multiple Channel
Single Channel
Fraction of Inertial flow at 1 A/cm²
0.5
0.4
0.3
0.2
0.1
0
24 AA
24 BA
28 AA
34 BA
24 BC
28 BC
34 BC
38 BC
GDL Types

Figure 7

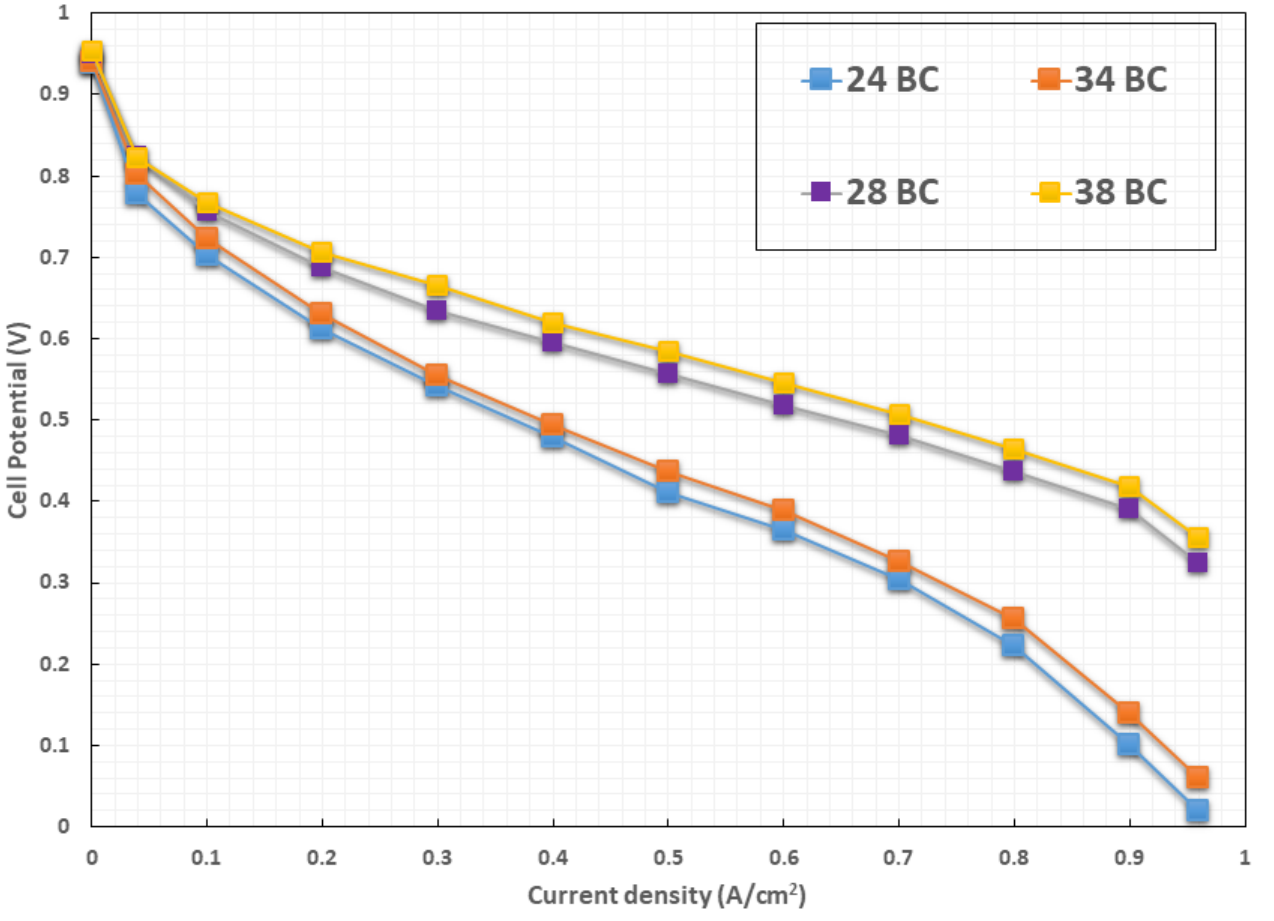
24 BC
34 BC
28 BC
38 BC
Cell Potential (V)
Current density (A/cm²)
0
0.1
0.2
0.3
0.4
0.5
0.6
0.7
0.8
0.9
1

Figure 8